

Accuracy of standard clinical 3T prostate MRI
for pelvic lymph node staging:
Comparison to ⁶⁸Ga-PSMA PET-CT

Sebastian Meißner¹; Jan-Carlo Janssen¹; Vikas Prasad², MD; Gerd Diederichs¹, MD; Bernd Hamm¹ MD, PhD; Winfried Brenner², MD, PhD; Marcus R. Makowski¹, MD, PhD.

¹ Department of Radiology, Charity, Charitéplatz 1, 10117 Berlin, Germany.

² Department of Nuclear Medicine, Charité, Charitéplatz 1, 10117 Berlin, Germany.

Manuscript category: Original article

Sebastian Meißner

Department of Radiology,

Charité Universitätsmedizin Berlin, Berlin, Germany.

sebastian.meissner@charite.de

phone: +49 30 450 645373

Supplementary data

Detection of lymph node metastasis in MRI dependent on lymph node size

To assess a possible impact of LN size in MRI detection, 2 groups were defined using the LAdm cut-off at 10mm in CT. For all LN, that were observed in PET-CT and MRI, the LN area was marginally larger in CT than in MRI. On average, the LN area in the MRI comprised 95.5% of the CT area and did not change significantly with longer delay between both scans ($\chi^2(2)=5.5$, $p=0.06$). patients with the shortest delay presented a congruence of 96.6 while patients with the longest delays had 93.8%. LN with a LAdm ≤ 10 mm in CT were detected with a sensitivity, specificity, PPV and NPV of 69.4% (CI 54.5%-81.1%), 99.5% (CI 99.0%-99.7%), 74.0% (CI 43.3%-91.4%) and 99.5% (CI 98.1%-99.9%) in MRI. They had a mean area of $0.4 \pm 0.3 \text{cm}^2$ (range 0.1–1.6 cm^2) and a mean size ratio of 0.9 ± 0.4 (range 0.3-3.5) in MRI. False negative LN had a mean area, size ratio and SUVmax of $0.4 \pm 0.3 \text{cm}^2$ (range 0.1–1.8 cm^2), 0.7 ± 0.1 (range 0.5–1.0) and 5.8 ± 3.8 (range 1.3-18.9) in ^{68}Ga -PSMA-PET-CT. False positive LN had a mean area of $1.1 \pm 0.7 \text{cm}^2$ (range 0.2-3.0 cm^2) and a size ratio of 0.7 ± 0.2 (range 0.4-1.0) in MRI. LN with LAdm > 10 mm in CT were detected with a sensitivity, specificity, PPV and NPV of 92.0% (CI 83.0%-96.5%), 95.6% (CI 90.2%-98.1%), 72.9% (CI 48.8%-88.4%) and 99.7% (CI 99.2%-99.9%) in MRI. They had a mean area of $1.4 \pm 1.5 \text{cm}^2$ (range 0.1-9.1 cm^2) and a size ratio of 0.8 ± 0.5 (range 0.3–3.4). False negative LN metastases had mean area, size ratio and SUVmax of $0.7 \pm 0.4 \text{cm}^2$ (range 0.4–1.6 cm^2), 0.6 ± 0.1 (range 0.4–0.8) and 7.0 ± 3.8 (range 0.7–10.4) in ^{68}Ga -PSMA-PET-CT. False positive LN had a mean area of $1.3 \pm 0.7 \text{cm}^2$ (range 0.3–3.0 cm^2) and a size ratio of 0.9 ± 0.1 (range 0.5-0.9) in MRI.

Overall, sensitivity in MRI did not differ significantly for both size groups ($\chi^2(1)=0.62$, $p=0.43$) although sensitivity in the ≤ 10 mm group (69%) tended to be lower than in the > 10 mm group (92%). More details are provided in supplementary table 1.

T1+T2	N	LN Size	Sensitivity + 95 % CI	Specificity + 95 % CI	PPV + 95 % CI	NPV + 95 % CI	p - value (accuracy)
LN	146 / 187	All	81.6 % (71.1 % - 88.9 %)	98.6 % (97.6 % - 99.2 %)	73.5 % (52.1 % - 87.6 %)	99.5 % (98.8 % - 99.8 %)	
	60 / 92	≤ 10mm	69.4 % (54.5 % - 81.1 %)	99.5 % (99.0 % - 99.7 %)	74.0 % (43.3 % - 91.4 %)	99.5 % (98.1 % - 99.9 %)	p = 0.301
	86 / 95	> 10mm	92.0 % (83.0 % - 96.5 %)	95.6 % (90.2 % - 98.1 %)	72.9 % (48.8 % - 88.4 %)	99.7 % (99.2 % - 99.9 %)	
Iliac left	7 / 13	≤ 10mm	63.2 % (33.2 % - 85.6 %)	99.3 % (97.6 % - 99.8 %)	49.3 % (7.0 % - 92.6 %)	99.7 % (96.1 % - 100 %)	p = 0.088
	16 / 18	> 10mm	92.0 % (68.7 % - 99.0 %)	89.0 % (60.1 % - 98.0 %)	53.0 % (16.4 % - 87.0 %)	99.0 % (94.6 % - 100 %)	
Iliac right	5 / 15	≤ 10mm	35.4 % (13.4 % - 65.8 %)	99.1 % (96.8 % - 99.7 %)	62.5 % (10.1 % - 96.1 %)	99.2 % (89.3 % - 99.9 %)	p = 0.715
	25 / 32	> 10mm	80.0 % (59.0 % - 92.0 %)	83.0 % (63.2 % - 93.0 %)	77.0 % (36.7 % - 95.0 %)	96.0 % (81.4 % - 99.0 %)	
Obturator left	14 / 19	≤ 10mm	72.1 % (42.9 % - 89.9 %)	98.2 % (94.0 % - 99.4 %)	61.5 % (12.0 % - 94.9 %)	98.6 % (86.0 % - 99.9 %)	p = 0.193
	14 / 14	> 10mm	100 % (0 % - 100 %)	100 % (0 % - 100 %)	100 % (0 % - 100 %)	100 % (0 % - 100 %)	
Obturator right	23 / 31	≤ 10mm	78.6 % (57.9 % - 90.8 %)	97.3 % (93.0 % - 99.0 %)	86.6 % (36.5 % - 98.6 %)	96.9 % (73.5 % - 99.7 %)	p = 0.334
	21 / 21	> 10mm	100 % (0 % - 100 %)	100 % (0 % - 100 %)	96.0 % (57.1 % - 100 %)	100 % (0 % - 100 %)	
Presacral	8 / 11	≤ 10mm	75.4 % (40.2 % - 93.3 %)	100 % (0 % - 100 %)	99.7 % (0 % - 100 %)	95.4 % (0 % - 100 %)	p = 0.334
	5 / 5	> 10mm	100 % a	100 % a	100 % a	100 % a	
Inguinal	3 / 3	≤ 10mm	100 % (0 % - 100 %)	100 % (0 % - 100 %)	100 % (0 % - 100 %)	100 % (0 % - 100 %)	p = 1.0
	5 / 5	> 10mm	100 % (0 % - 100 %)	97.0 % (0 % - 100 %)	21.0 % (3.4 % - 67.0 %)	100 % (0 % - 100 %)	

a = CI could not be calculated as PET-CT and MRI agreed perfectly in this case.

Supplementary table 1. Size-based analysis of the detection rates using combined T1+T2+DWI sequence MRI evaluation

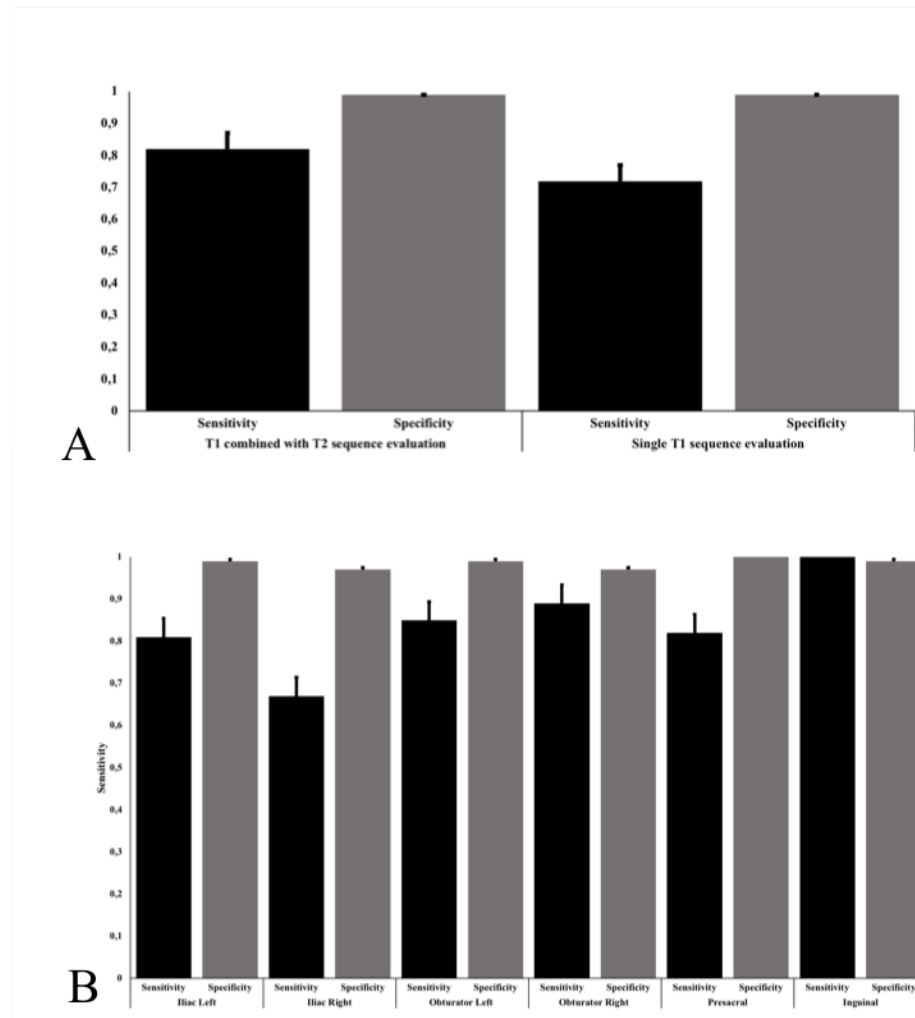
This table summarizes the size-based analysis of the lymph node metastases in MRI using T1 combined with T2 and DWI sequence evaluation. All ⁶⁸Gallium-Prostate membrane antigen PET-CT positive metastases were categorized in two subgroups with a long-axis diameter ≤10mm and >10mm measured in axial plane. The columns present the numbers of seen LN compared to PET-CT, sensitivities, specificities, positive and negative predictive value including 95% confidence interval and the p-values of differences in the accuracy of detection. The rows show the overall values of all found metastases ≤10mm and >10mm and fielded in the six defined anatomical regions iliac left and right, obturator left and right, presacral and inguinal region. A p-value p<0.05 was considered statistically significant.

When no confidence intervals could be calculated due to perfect agreement of MRI and PET-CT, it is highlighted in the table with an “a”.

Abbreviations: T2 = T2 weighted sequence, DWI = diffusion weighted imaging sequence, LN = Lymph nodes, N = number of positive LN in MRI versus PET-CT, PPV = positive predictive value, NPV = Negative predictive value, CI = 95% Confidence interval

Detection of lymph node metastasis in MRI dependent on size and anatomical region

Furthermore, the two size groups were examined based on the anatomical regions. No significant differences were seen throughout all anatomical regions. Although a tendency was seen for the iliac left region ($\chi^2(1)=2.9$, $p=0.08$). Further details are provided in supplementary figure 1.



Supplementary figure 1: Visualisation of the detection rates of lymph node metastases smaller and larger than 10mm in MRI

A: This bar chart presents the accuracy of the detection for lymph node (LN) metastases smaller 10mm versus larger than 10mm showing the overall sensitivities and specificities. No significant ($p>0.05$) difference in the accuracy was seen. B: This bar chart presents the accuracy of the detection for LN metastases smaller 10mm versus larger than 10mm on a region-based

analysis in the six defined anatomical regions iliac left and right, obturator left and right, presacral and inguinal region. No significance ($p>0.05$) was seen throughout all anatomical regions.

Abbreviations: LN = Lymph nodes

Impact of the additional T2 and DWI sequences in the detection of lymph node metastasis dependent on lymph node size

LN with a LAdm ≤ 10 mm in CT were detected in with a sensitivity, specificity, PPV and NPV of 73.7% (CI 56.9%-85.6%), 99.7% (CI 99.4%-99.9%), 77.8% (CI 45.1%-93.7%) and 99.6% (CI 99.3%-99.9%) in single T1 sequence evaluation. They had a mean area of $0.4\pm 0.3\text{cm}^2$ (range 0.1–1.6 cm^2) and a mean size ratio of 0.9 ± 0.1 (range 0.3-1.0) was in single T1 evaluation. False negative LN had a mean area, size ratio and SUVmax of $0.4\pm 0.3\text{cm}^2$ (range 0.1–1.8 cm^2), 0.7 ± 0.2 (range 0.5–1.5) and 5.8 ± 3.8 (range 1.3-18.9) in ^{68}Ga -PSMA-PET-CT. the 2 false positive LN had a mean area of $0.9\pm 0.7\text{cm}^2$ (range 0.2-3.0 cm^2) and a mean size ratio of 0.9 in single T1 evaluation. LN with LAdm >10 mm in CT were detected with a sensitivity, specificity, PPV and NPV of 70.0% (CI 52.6%-83.1%), 97.1% (CI 94.1%-98.6%), 69.8% (CI 43.0%-87.6%) and 99.1% (CI 97.2%-99.7%) in single T1 evaluation. They had a mean area of $1.3\pm 1.4\text{cm}^2$ (range 0.1-9.1 cm^2) and a size ratio of 0.7 ± 0.2 (range 0.3–1.0). False negative LN metastases had mean area, size ratio and SUVmax of $0.8\pm 0.3\text{cm}^2$ (range 0.4–1.6 cm^2), 0.6 ± 0.1 (range 0.4–0.8) and 6.8 ± 3.6 (range 0.7–12.8) in ^{68}Ga -PSMA-PET-CT. False positive LN had a mean area of $0.9\pm 0.3\text{cm}^2$ (range 0.6–1.3 cm^2) and a size ratio of 0.9 ± 0.2 (range 0.5-1.0).

Overall sensitivity in single T1 sequence evaluation did not differ significantly for both size groups since the sensitivity in the ≤ 10 mm group (73.7%) was only marginally higher than in the >10 mm group (70%) and most of the CI overlapped. The same non-significant effect was

seen in the assessment of sensitivity differences based on size and anatomical regions. More details are provided in supplementary table 1.

Single T1	N	LN Size	Sensitivity + 95 % CI	Specificity + 95 % CI	PPV + 95 % CI	NPV + 95 % CI
LN	130 / 187	All	81.6 % (71.1 % - 88.9 %)	98.6 % (97.6 % - 99.2 %)	73.5 % (52.1 % - 87.6 %)	99.5 % (98.8 % - 99.8 %)
	50/ 92	≤ 10mm	73.7 % (56.9 % - 85.6 %)	99.7 % (99.4 % - 99.9 %)	77.8 % (45.1 % - 93.7 %)	99.6 % (99.3 % - 99.9 %)
	80 / 95	> 10mm	70.0 % (52.6 % - 83.1 %)	97.1 % (94.1 % - 98.6 %)	69.8 % (43.0 % - 87.6 %)	99.1 % (97.2 % - 99.7 %)
Iliac left	5 / 13	≤ 10mm	75.0 % (43.6 % - 92.0 %)	100 % (81.7 % - 100 %)	42.0 % (3.9 % - 93.0 %)	100 % (98.0 % - 100 %)
	16/18	> 10mm	72.0 % (41.6 % - 90.0 %)	95.0 % (82.7 % - 98.0 %)	54.0 % (12.9 % - 90.0 %)	98.0 % (88.4 % - 100 %)
Iliac right	4 / 15	≤ 10mm	51.0 % (21.1 % - 80.0 %)	100 % (98.8 % - 100 %)	90 % (10.2 % - 100 %)	100 % (81.7 - 100 %)
	24 / 32	> 10mm	71.0 % (46.1 % - 87.0 %)	87.0 % (69.4 % - 95.0 %)	72.0 % (28.2 % - 95.0 %)	95.0 % (74.5 % - 99.0 %)
Obturator left	13 / 19	≤ 10mm	80.0 % (48.5 % - 94.0 %)	100 % (97.8 % - 100 %)	90.0 % (15.9 % - 100 %)	100 % (82.0 % - 100 %)
	11 / 14	> 10mm	69.0 % (29.3 % - 93.0 %)	100 % (0 % - 100 %)	100 % (0 % - 100 %)	45.0 % (0 % - 100 %)
Obturator right	17 / 31	≤ 10mm	74.0 % (51.2 % - 89.0 %)	98.0 % (95.0 % - 99.0 %)	73.0 % (16.2 % - 97.0 %)	98.0 % (78.4 % - 100 %)
	19 / 21	> 10mm	56.0 % (28.8 % - 80.0 %)	93.0 % (80.4 % - 98.0 %)	95.0 % (40.1 % - 100 %)	36.0 % (1.9 % - 94.0 %)
Presacral	8 / 11	≤ 10mm	77.0 % (41.1 % - 94.0 %)	100 % (0 % - 100 %)	100 % (0 % - 100 %)	98.0 % (0 % - 100 %)
	5 / 5	> 10mm	100 % a	100 % a	100 % a	100 % a
Inguinal	3 / 3	≤ 10mm	100 % (0 % - 100 %)	100 % (0 % - 100 %)	100 % (0 % - 100 %)	100 % (0 % - 100 %)
	5 / 5	> 10mm	100 % (0 % - 100 %)	98.0 % (0 % - 100 %)	20.0 % (2.5 % - 71.0 %)	100 % (0 % - 100 %)

a = CI could not be calculated as PET-CT and MRI agreed perfectly in this case.

Supplementary table 2. Size-based analysis of the detection rates using single T1 sequence MRI evaluation

This table summarizes the size-based analysis of the lymph node metastases in MRI using single T1 sequence evaluation. All ⁶⁸Gallium-Prostate membrane antigen PET-CT positive metastases were categorized in two subgroups with a long-axis diameter ≤10mm and >10mm measured in axial plane. The columns present the numbers of seen LN compared to PET-CT, sensitivities, specificities, positive and negative predictive value including 95% confidence intervals. The rows show the overall values of all found metastases ≤10mm and >10mm and fielded in the six defined anatomical regions iliac left and right, obturator left and right, presacral and inguinal region.

When no confidence intervals could be calculated due to perfect agreement of MRI and PET-CT, it is highlighted in the table with an “a”.

Abbreviations: LN = Lymph nodes, N = number of positive LN in MRI versus PET-CT, PPV = positive predictive value, NPV = Negative predictive value, CI = 95% Confidence interval

References

- 1 Prasad V, Steffen IG, Diederichs G, Makowski MR, Wust P, Brenner W (2016) Biodistribution of [(68)Ga]PSMA-HBED-CC in Patients with Prostate Cancer: Characterization of Uptake in Normal Organs and Tumour Lesions. *Mol Imaging Biol* 18:428-436
- 2 Dietlein M, Kobe C, Kuhnert G et al (2015) Comparison of [(18)F]DCFPyL and [(68)Ga]Ga-PSMA-HBED-CC for PSMA-PET Imaging in Patients with Relapsed Prostate Cancer. *Mol Imaging Biol* 17:575-584
- 3 Afshar-Oromieh A, Malcher A, Eder M et al (2013) PET imaging with a [68Ga]gallium-labelled PSMA ligand for the diagnosis of prostate cancer: biodistribution in humans and first evaluation of tumour lesions. *Eur J Nucl Med Mol Imaging* 40:486-495
- 4 Surti S, Kuhn A, Werner ME, Perkins AE, Kolthammer J, Karp JS (2007) Performance of Philips Gemini TF PET/CT scanner with special consideration for its time-of-flight imaging capabilities. *J Nucl Med* 48:471-480